

# Magnetic Properties of Nanowires guided by Carbon Nanotubes

Miguel A. Correa-Duarte and Veronica Salgueirino  
*Universidade de Vigo  
Spain*

## 1. Introduction

The physical properties of one-dimensional (1D) nanostructures of magnetic materials are presently the subject of intensive research, taking into account the considerable attention they have recently received and the few cases reported. [1-4] Much of the early work was concerned with exploratory issues, such as establishing an easy axis for typical preparation conditions and the essential involvement of shape anisotropy, as opposed to magnetocrystalline anisotropy. More recently, attention has shifted towards the understanding of magnetization processes and related applications. Particularly interesting problems are the magnetic hysteresis of the wires and the time dependence of the magnetic reversal. Thus, magnetic nanowires have provided a highly successful test ground for understanding the microscopic mechanisms that determine macroscopically important parameters in the different applications where they can be used. [5]

On the other hand, these building blocks, as in the case of spherical nanoparticles, are at the border between the solid and molecular state displaying the novel effects that can now be exploited. Therefore, it becomes imperative to take into account the fact that the properties of materials composed of magnetic nanostructures are a result of both the intrinsic properties of the small building blocks and the interactions in between. [6]

This chapter is not meant as a survey of the present state and future developments of magnetic nanowires and since only two examples are considered, is far from being complete. The purpose of this chapter is three fold: a) an introductory level overview about magnetic colloids, the basic physics in the magnetism at the nanoscale; in terms of superparamagnetism, the concept of magnetic anisotropy and the dynamics of these systems. We have emphasized the dominant role of the surface effects on the intrinsic properties at the nanoscale and the competition with the interactions in the case of assemblies, leading to a characteristic magnetic behavior termed as *spin-glass*. Additionally, a brief introduction referred to carbon nanotubes (CNTs) is included. b) Characteristic examples of magnetic nanowires whose morphology was achieved by taking advantage of CNTs and exploiting wet-chemistry methods, and c) a complete analysis of the magnetic behavior displayed in both examples.

### 1.1 Colloids

Different preparation methods lead to magnetic nanostructures with differences in crystalline structure, surface chemistry, shape, etc. Hence, the fabrication technique has a

Source: Nanowires Science and Technology, Book edited by: Nicoleta Lupu,  
ISBN 978-953-7619-89-3, pp. 402, February 2010, INTECH, Croatia, downloaded from SCIYO.COM

great influence on the magnetic properties of the materials obtained. Numerous physical and chemical methods have been employed to produce magnetic nanostructures, such as *molecular beam epitaxy*, *chemical vapor deposition*, *normal incident pulsed laser deposition*, *sputtering* or *electrodeposition*. The magnetic colloidal nanostructures or colloids are remarkably different if compared to nanostructures formed by these methods, as they are chemically synthesized using wet chemistry and are free-standing nanocrystals grown in solution. [7] The magnetic colloids are thus a subgroup of a broader class of the magnetic materials that can be synthesized at the nanoscale level but using wet chemical methods. In this fabrication of colloidal nanocrystals, the reaction chamber is a reactor containing a liquid mixture of compounds that control the nucleation and the growth. In general, each of the atomic species that will be part of the nanostructures is introduced into the reactor in the form of a precursor. A precursor is a molecule or a complex containing one or more atomic species required for growing the nanocrystals. Once the precursors are introduced into the reaction flask they decompose, forming new reactive species (the monomers) that will cause the nucleation and growth of the nanocrystals. The liquid in the reactor provides the energy required to decompose the precursors, either by thermal collisions or by a chemical reaction between the liquid medium and the precursors, or by a combination of these two mechanisms. [8] The key parameter in the controlled growth of colloidal nanocrystals is the presence of one or more molecular species in the reactor that we will term as *ligands* hereafter. A ligand is a molecule that is dynamically adsorbed to the surface of the growing structure under the reaction conditions. It must be mobile enough to provide access for the addition of monomer units, while stable enough to prevent the aggregation of nanocrystals in solution. Figure 1 provides a schematic illustration of a nanostructure with an example of a mobile ligand adsorbed on its surface. Due to the increased surface-to-volume ratio, surface chemistry is of great importance for the chemical and physical properties of the colloids likewise synthesized, generally being caused by these molecular ligands stabilizing them.

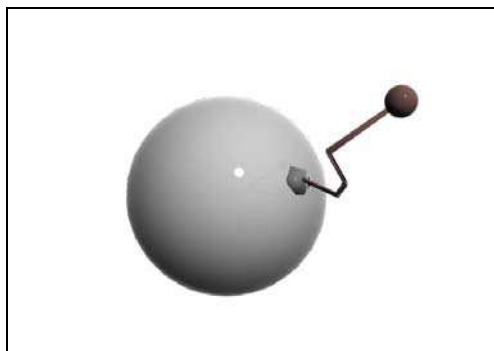


Fig. 1. Schematic illustration of a nanostructure with an example of a mobile ligand adsorbed on its surface.

The preparation of nanostructures of desired sizes is the first and very important step, being a prerequisite of their further investigation and use. Narrow size distribution or monodispersity is highly desirable because magnetic properties become strongly size dependent in the nanometer size range. Additionally, the magnetic behavior of nanostructures depends not only on their chemical composition and size, but also on their crystalline modification and the presence of structural defects like stacking faults or twinned

planes. Consequently, Murray *et al.* proposed the use of the term “nanocrystal” for crystalline particles with low concentrations of defects, while the more general term “nanoparticle” also includes particles containing gross internal grain boundaries, fractures, or internal disorder. [9] Another important characteristic of the wet-chemistry methods refers to the fact that the colloids are dispersed in solution, and so that, they can be produced in large quantities in a reaction flask and can later be transferred to any desired substrate.

## 1.2 Superparamagnetism

It is well known that a magnetic body has a structure that is divided into uniformly magnetized regions (domains) separated by domain or Bloch walls. This distribution of regions or domains permits the magnetic body to minimize its magnetostatic energy. Since it is the total energy that requires to be minimized, it will be a final balance of energies (including the magnetostatic and the exchange terms, the different anisotropies that come into play and the domain walls contribution) what will determines the domain structure. In order to work at the nanoscale, there will be an important reduction in dimensions, so that, the size of the domains will also be reduced. At this point, the domain structure will consequently change, but due to the domain wall formation energy cost, the balance with the magnetostatic energy will limit the subdivision in domains to a certain optimum size. Consequently, there is a size limit below which the nanostructure can no longer gain an energy favorable configuration by breaking up into domains. Hence, it remains with only one domain. The critical size, or single domain size  $D_s$ , below which a particle will not form domains, is where these two energies (energy cost of domain walls formation and magnetostatic energy) become equal, and the typical values for  $D_s$  range from 10 to 100 nm, with elongated nanostructures tending to have larger  $D_s$ .

Much of the behavior of these single-domain magnetic nanostructures can be described by assuming that all the atomic moments are rigidly aligned as a single “giant” spin. This is in essence the theory of superparamagnetism. Below the Curie temperature of a ferromagnet or ferrimagnet, all the spins are coupled together and so cooperate to yield a large total moment  $\mu$  (the giant spin). This moment is bound rigidly to the nanostructure by one or more of the variety of anisotropies (that will be later discussed). The energy of this bond is  $KV$ , where  $K$  is the effective magnetic anisotropy (that takes into account the variety of anisotropies that come into play) and  $V$  is the volume of the particle. With decreasing size, the  $KV$  magnitude decreases and the thermal energy  $kT$  can disrupt the bonding of the total magnetic moment to the nanostructures. The magnetic moment in this situation is free to move and respond to an applied field independently of the nanostructure itself. An applied field would tend to align it, but  $kT$  would fight the alignment just as it does in a paramagnet (justifying therefore the use of the term superparamagnet). [10]

The phenomenon of superparamagnetism is, in fact, timescale-dependent due to the stochastic nature of the thermal energy  $kT$ . The anisotropy energy  $KV$  represents an energy barrier to the total spin reorientation, hence the probability for jumping this barrier is proportional to the Boltzmann factor  $\exp(-KV/kT)$ . This can be made quantitative by introducing an attempt timescale,  $\tau_0$  which describes the timescale over which  $\mu$  attempts to jump the  $KV$  barrier. Then, the timescale for a successful jump is

$$\tau = \tau_0 e^{-KV/kT} \quad (1)$$

The attempt timescale is about  $10^{-9}$  s. The typical experiment with a magnetometer takes 10 to 100 s; and if  $M_s$  reverses at times shorter than the experimental timescale, the system appears superparamagnetic. Thus, using  $\tau \approx 100$  s and  $\tau_0 = 10^{-9}$  s, the critical volume becomes:

$$V_{sp} = \frac{25kT}{K} \quad (2)$$

$$T_B = \frac{KV}{25k} \quad (3)$$

The equation (2) can be rearranged to yield equation (3) and gives the blocking temperature  $T_B$ . Below  $T_B$  the free movement of  $\mu = M_s V$  is blocked by the anisotropy; above  $T_B$ ,  $kT$  permits the magnetic moment ( $\mu$ ) to fluctuate freely, so that the system appears superparamagnetic.

### 1.3 Magnetic anisotropy

The magnetic anisotropy concept describes the fact that the energy of the ground state of a magnetic system depends on the direction of the magnetization. The effect occurs either by rotations of the magnetic moment  $\mu$  with respect to the external shape of the specimen (shape anisotropy) or by rotations relative to the crystallographic axes (intrinsic or magnetocrystalline anisotropy). The direction(s) with minimum energy, i.e. into which the magnetic moment  $\mu$  points in the absence of external fields are called easy directions. The direction(s) with maximum energy are called hard directions. The magnetic anisotropy energy (MAE) between two crystallographic directions is given by the work needed to rotate the magnetic moment  $\mu$  from an easy direction into the other directions. The MAE, that corresponds to a small contribution to the total energy of a bulk crystal, becomes more and more important as decreasing the size of the magnetic material until reaching the nanoscale, depending on different issues.

In bulk materials, magnetocrystalline and magnetostatic energies are the main sources of anisotropy, but in nanosized structures, other types of anisotropy can be of the same order of magnitude. As the properties are stated by the relaxation time  $\tau$  of the magnetic moment  $\mu$  on the nanostructures,  $\tau$  being itself governed by the energy barrier  $KV$  (directly dependent on the effective magnetic anisotropy  $K$ ), it is important to know all the possible sources of anisotropies and their contribution to the total energy barrier.

There are fundamentally two sources of magnetic anisotropy; (i) spin-orbit (LS) interaction and (ii) the magnetic dipole-dipole interaction. The more important interaction is the spin-orbit coupling, which couples the spin to the charge (orbital) density distribution in the crystal. Thus, the magnetic moment  $\mu$  "gets the feel" of the crystal via the orbital motion of the magnetic electrons. The orbital motion is coupled to the lattice by an electric field (that indeed reflects the symmetry of this lattice). This field  $K$  is given by the sum of the electrostatic potentials  $\phi(r_i)$  over the nearest neighbors at sites  $r_i$ . [11]

$$K = \sum_i^N e \cdot \phi(|\vec{r}_i|) \quad (4)$$

The first source (spin-orbit) of magnetic anisotropy includes the so-called magneto-crystalline and magneto-elastic contributions while the second one (from magnetic dipole-dipole interactions) includes contributions termed shape or magneto-static anisotropy. [12] Accordingly, when considering the nanoparticulate systems, there are main contributions referred to the magnetocrystalline anisotropy whose energy can show various symmetries (uniaxial and cubic forms cover the majority of the cases), to the surface anisotropy (related to surface effects that stem from the fact that the existence of the surface represents a discontinuity for magnetic interactions) and to magnetostatic energy. Additionally, stress anisotropy should be taken into account as well since there is a second effect due to the surface, related to strains, because of a magnetostriction effect. [13]

If we refer to the magnetocrystalline anisotropy, the direction of the spontaneous magnetization of crystalline samples is oriented along certain directions. Typically, for bulk samples of bcc-Fe, fcc-Ni, and hcp-Co, these are the cubic  $\langle 100 \rangle$ ,  $\langle 111 \rangle$  and hexagonal  $\langle 0001 \rangle$  directions, respectively. These directions are called easy magnetization directions and the magnetization along any other direction requires an excess energy. [14] The magnetic anisotropy energy density is indeed the excess work that needs to be put into the system to achieve saturation magnetization along a non-easy axis of magnetization. This excess work depends on the orientation of the magnetizing field with respect to the sample, and its magnitude will be different in general for magnetization in the different directions of the crystalline lattice. In sharp contrast to the small crystalline anisotropy of bulk samples, ultrathin films and nanostructures often exhibit an effective magnetic anisotropy that is orders of magnitude larger than the respective bulk value. The deviation from the respective bulk values has been ascribed in most cases to a magnetocrystalline surface anisotropy of the Néel type. [15]

In general, one can always apply the rule that indicates that the lower the symmetry of the crystals or of the local electrostatic potential around the magnetic moment, the larger the MAE is. [16] The mentioned increase of magnetic anisotropy for ultrathin films and nanostructures is often ascribed to so-called interface and surface anisotropy contributions that are attributed to the different atomic environment of the interface and surface atoms, where the symmetry of the crystals is much lower than in internal positions. [12]

The important impact of symmetry on the resulting magnetic anisotropy can also be understood in the crystal field description, which has been applied successfully to describe the magnetic anisotropy of 3d ions. [17] The energetically degenerate 3d levels of a free atom split into two groups,  $e_g$  ( $d_{z^2}$ ,  $d_{x^2-y^2}$  orbitals) and  $t_{2g}$  ( $d_{xy}$ ,  $d_{xz}$  and  $d_{yz}$  orbitals) in the presence of the electric field of the surrounding atoms. The energy separation and the relative positioning of the  $e_g$  and  $t_{2g}$  levels depend on the symmetry of the atomic arrangement [18] and a tetragonal distortion lifts the degeneracy of these levels. [19] Thus, a change of symmetry, e.g. induced by strain, may lead to a change of the relative occupancy of the different d-orbitals, which in turn leads via spin-orbit coupling to a change of the magnetic anisotropy.

In order to illustrate the role of the symmetry (and surface effects) we can consider the following case. At each lattice point within for example, a cubic lattice, the dipole fields of all neighbors cancel out. This is, however, only true for an infinite system. As soon as surfaces are present, magnetic poles develop and thus, the dipole-dipole interaction leads to anisotropy. Since the shape of the sample determines this anisotropy (even for modest shape ratios  $c/a$ , the shape anisotropy can be very large), one usually calls it shape anisotropy. As a

result, in systems with reduced dimensions as nanostructures, the shape anisotropy might be even the dominating contribution to the overall MAE. [16]

Another important contribution comes from a well-known experimental fact derived from the coupling between magnetism and lattice strain, the magnetostriction, which origins the magnetoelastic anisotropy. A sample lowers its total energy upon magnetization by a lattice strain that depends on the magnetization direction with respect to the crystalline lattice. The underlying principle of the so-called magnetoelastic coupling can be described as the strain dependence of the magnetic anisotropy energy density. [20] For thin films and nanostructures, since are generally under considerable strain, this contribution can also determine the magnetic anisotropy.

Cantilever bending experiments and nanoindentation techniques are sensitive and accurate tools for the measurement of mechanical stress in atomic layers, at surfaces and on nanoparticles. The idea of the measurement in the former case is to detect the stress-induced change in curvature of a thin substrate. The curvature change is directly proportional to the film stress, integrated over the film thickness. The second case, the nanoindentation, has now long been used to study the elastic, plastic, and fracture properties of surfaces of bulk samples, and in the last decade, it has become possible to perform controlled compression and bending tests on nanostructures smaller than a micron, such as NPs, [20-24] nanowires [25-26] and nano-pillars. [27-28] In both cases, the elastic properties of the magnetic structures are given by the Young's modulus and the Poisson ratio and the magnetoelastic coupling coefficients can then be derived.

Although the important aspect of magnetic domain formation is not discussed here since we have restricted the scope of the introduction to theoretical single-domain nanostructures behavior, we will actually take into account the interplay of magnetostatic energy, exchange energy and the effective magnetic anisotropy that can lead to an energetically favored multi-domain state. Hence, aspects of configurational magnetic anisotropy that appear in submicron-sized magnets due to small deviations from the uniform state [29] and the so-called exchange anisotropy are considered.

The phenomenon of exchange anisotropy is the result of an interfacial exchange interaction between ferromagnetic (FM) and antiferromagnetic (AFM) materials, and only recently have the required experimental and analytical tools for dealing with interfacial behavior at the atomic level become available. [30] The observation (below room temperature) of a hysteresis loop shifted along the field axis, after cooling a nanostructured system in an applied field, indicates an exchange interaction across the interface between a FM and an AFM materials composing the sample. This loop shift was demonstrated to be equivalent to the assumption of a unidirectional anisotropy energy in the expression for the free energy at  $T=0K$  of single-domain spherical particles with uniaxial anisotropy, aligned with their easy axis in the direction of the field,  $H$ , which is applied anti-parallel to any particle's magnetization  $M_s$ :

$$F = HM_s \cos \theta - K_u \cos \theta + K_l \sin^2 \theta \quad (5)$$

where  $\theta$  is the angle between the easy direction and the direction of magnetization, and  $K_u$  and  $K_l$  are the unidirectional and uniaxial anisotropy energy constants, respectively. Solutions of this equation are readily expressed in terms of an effective field  $H'$ ,

$$H' = H - \frac{K_u}{M_s} \quad (6)$$

that offers the hysteresis loop displaced by  $K_u/M_s$ , on the  $H$ -axis. Thus, an explanation of the loop shift is equivalent to explaining the unidirectional anisotropy.

AFM materials appear magnetically ordered below their Néel temperatures  $T_N$ , and have a zero net moment since have parallel and anti-parallel spins in a preferred direction. However, at the interface with a FM, there are localized net moments that arise from several sources. Indeed, in AFM nanostructures with compensated interfacial spin planes, there can be unequal numbers of parallel and antiparallel spins at the surface of the nanostructure, due to various origins such as its size, shape or roughness, generating localized net AFM moments. Since the FM is ordered at its Curie temperature  $T_C$ , greater than the  $T_N$  of the AFM, a field applied to couple FM-AFM systems at  $T > T_N$  will align the FM magnetization in the field direction, while the AFM spins remain paramagnetic. As the temperature is lowered through  $T_N$ , the ordering net localized AFM spins will couple to the aligned FM spins, sharing their general spin direction. For high AFM magnetocrystalline anisotropy, if the interfacial AFM spins are strongly coupled to the AFM lattice, they will not be substantially rotated out of their alignment direction by fields applied at temperatures below  $T_N$ . However, since the localized uncompensated AFM spins are coupled to FM spins at the interface, they exert a strong torque on these FM spins, tending to keep them aligned in the direction of the cooling field, i.e., a unidirectional anisotropy.

Skumryev *et al.* demonstrated a magnetic coupling of FM nanoparticles with an AFM matrix as a source of a large effective additional anisotropy that led to a marked improvement in the thermal stability of the moments of the FM nanoparticles. The mechanism provides a way to beat the “*superparamagnetic limit*” in isolated particles so that, with the right choice of FM and AFM components, exchange anisotropy coupling could ultimately allow magnetically stable nanostructures. These nanostructures, only a few nanometers in size, would be able to surpass the storage-density goal of 1 *Tbit in*<sup>2</sup>, as set by the magnetic storage industry. [31]

As stated, the surface anisotropy is expected to contribute decisively for systems dominated by their surface properties, e.g. nanostructures offering an increased surface/volume ratio as it is the case of the magnetic colloids discussed here. Indeed, when it comes to magnetic nanostructures, the dominant surface contributions stem from the decisive role of ligands coverage onto the surface of the nanoparticles in order to render them dispersable in different solvents (colloidal chemistry), and therefore, became relevant for the resulting magnetic anisotropy. Experimental and theoretical reports have identified this decisive role of the ligands or molecular compounds adsorbed on the surface of different nanostructures in their magnetic anisotropy. [32] Since small structural relaxations can be induced by these ligands due to an induced spin reorientation related to the magnetoelastic coupling, it can be concluded that this magnetoelastic coupling opens the way to influence the magnetic anisotropy by even subtle structural and chemical changes at the surface. [33-36] Thus, surface magnetic properties result basically from the breaking of symmetry of the lattice, [37,38] which leads to site-specific, generally uniaxial, surface anisotropy, and from broken exchange bonds, which inevitably lead to surface spin disorder and frustration (most prominently in oxydic ferro-, antiferro- and ferrimagnets). [39,40]

On the other hand, the coordination of the ligands to the nanostructures surface should not alter the intrinsic specific physical properties of the particles nor those induced by their nanometer size. This latter point is important in order to take advantage of both the intrinsic and collective properties for future applications. Dumestre *et al.* have reported an

organometallic route towards the synthesis of metallic nanoparticles that can be applied to magnetic ones, based on the decomposition of an olefinic complex under a controlled atmosphere of  $H_2$  in mild conditions of pressure. [41] Respaud *et al.* were able to demonstrate that the surface of this type of nanoparticles is free of contaminating agents so that, the magnetic properties are identical to those observed for nanoparticles produced and studied in ultra high vacuum. [42]

The magnetic anisotropy of magnetic nanostructures can therefore be tuned by a proper selection of the combination between the magnetic material itself and the molecular ligands attached to their surface to stabilize them, and by adjusting the growth parameters in the synthetic process used (herein we refer specifically to colloidal chemistry methods). Thus, the link between growth parameters and magnetism is given by the correlation between the nanostructures morphology, structure and the magnetic properties themselves. This correlation is given by the magnetoelastic coupling, and by the length scale of structure and morphological variations as compared to the length scale that describes magnetic properties. Such a magnetic length scale is for example, the domain wall, the exchange stiffness or the magnetic anisotropy. [12]

Additionally, despite the fact that we have just introduced single-domain nanostructures, if we consider the magnetization reversal by domain motion, an impact of structural and magnetic anisotropy variations on the coercivity will be expected. These variations should occur on a length scale larger than the domain wall width otherwise the magnetic inhomogeneities will be average out by the magnetic exchange interactions, and only little impact will result on the coercivity. [43]

#### 1.4 Collective magnetic behavior

One of the most attractive topics in the field of condensed matter physics is slow dynamics such as nonexponential relaxation, aging (a waiting time dependence of observables) and memory effects. In the field of spin glasses, slow dynamics has been studied widely both experimentally and theoretically to examine the validity of novel concepts, such as a hierarchical organization of states and temperature chaos. These extensive studies have revealed interesting effects like memory and rejuvenation [44, 45] that led to also study slow dynamics in dense magnetic nanoparticulate systems by using experimental protocols already developed.

In the case of magnetic nanostructures systems, there are two possible origins of slow dynamics. The first one is a broad distribution of relaxation times originating solely from that of the anisotropy energy barriers of each nanoparticle moment. This is the only source of slow dynamics for sparse (weakly interacting) magnetic nanoparticle systems, in which the nanoparticles are fixed in space. However, for dense magnetic nanoparticle systems, there is a second possible origin of slow dynamics, namely, cooperative spin-glass dynamics due to frustration caused by strong dipolar interactions among the particles and randomness in the particle positions and anisotropy axis orientations. [46, 47] The 3D random distributions and random orientations of anisotropy axes of such nanostructures in an insulating matrix with high enough packing density and sufficiently narrow size distribution will create a competition of different spin alignments. [48] Which of the two is relevant depends essentially on the concentration of the particles. Therefore, in order to understand appropriately slow dynamics in magnetic nanoparticle systems, it is desirable to clarify both.



The comparison of the phenomena observed in relation to slow dynamics reveals some properties peculiar only to spin glasses, e.g. the flatness of the field-cooled magnetization below the critical temperature and memory effects in the zero-field-cooled magnetization. These two effects reflect the instability of the spin-glass phase under a static magnetic field of any strength meaning that it is indeed far from equilibrium. [49]

The intriguing properties of magnetic nanostructures including superparamagnetic and spin glass behavior are often ascribed to the delicate interplay between intrinsic properties and magnetostatic interactions.[50] When comparing between superparamagnets and spin-glass-like behavior of nanostructures, one significant difference is seen in the  $M_{FC}$  without intermittent stops (when cooling the system). While in the case of superparamagnets this  $M_{FC}$  increases as decreasing temperature, in the second case, the nearly constant  $M_{FC}$  is actually considered to be a typical property of ordinary spin glasses. Additionally, a further important phenomenon that is peculiar to superspin-glasses is the memory effect in the genuine ZFC protocol. This memory experiment in a ZFC protocol permits to differentiate between spin-glass phase and superparamagnets interacting. In this experiment,  $M_{ZFC}$  is measured with and without stops and in both cases cooling (and reheating) rate has to be the same. The stopping temperatures must be well below the blocking temperature  $T_B$  of the system measured. The results of the experiment will give us no significant difference in  $M_{ZFC}$  at the stopping temperatures and below when considering magnetic nanostructures weakly interacting. In this case then, the origin of slow dynamics is without doubt the broad distribution of relaxation times originating solely from the distribution of magnetic anisotropy energies of the nanostructures considered. On the contrary, if there is a significant difference in  $M_{ZFC}$  at the stopping temperatures and below, we must now consider our system of magnetic nanostructures as offering a spin-glass-like behavior.

It is important to carry out this latter experiment considering the  $M_{ZFC}$  and not the  $M_{FC}$  since only a spin glass left unperturbed by external fields at constant  $T$ , rearranges its spin configuration through a very slow process to reduce the domain wall energy. [51] Indeed, all measurements should be done in quite low magnetic fields in order to avoid nonlinear effects.<sup>48</sup> Moreover, Jonsson *et al.* reported that the collective behavior due to dipole-dipole interactions in concentrated samples extended the magnetic relaxation towards longer times and at the same time suppressed the relaxation at short observation times, a behavior that conforms to characteristic spin glass dynamics. [52]

One more point to be concerned about is the fact that collective magnetic excitations account for the precession or oscillations of the magnetic moment in the nanostructure about its magnetic easy axis, triggered at low temperatures by thermal energies insufficient to induce spin flips between opposite directions of the anisotropy axis, for  $k_B T < K_{eff} V$ . However, the particle surface-energy landscape can accommodate additional local minima due to lower coordination of the surface atoms, surface strain and spin canting associated with the surface itself. Many studies indicate that the breakage of superexchange bonds results in the creation of a surface shell within which spin disorder leads to spin-glass-like phase at the surface with closely spaced equilibrium states. [39, 53]

### 1.5 Carbon nanotubes

A great example representing the ever-increasing nanoscale-based research refers to the sp<sup>2</sup>-bonded carbon nanotubes (CNTs) discovered in 1991. [54] CNTs have been pointed out as a paradigm material when talking about Nanotechnology. This new form in the carbon family

with remarkable structure-dependent electronic, mechanical, optical and magnetic properties [55] has been the focus of an intensive study directed to numerous applications on many different fields, [56, 57] including synthetic routes where CNTs are useful for biological applications. [58, 59] Therefore, CNTs are expected to be controllably assembled into designed architectures as integral components of composites and/or supramolecular structures.

CNTs are hollow cylinders consisting of single or multiple sheets of wrapped graphite. According with the number of layers they are classified as single-walled carbon nanotubes (SWNTs) or multi-walled carbon nanotubes (MWNTs). Usually the structure of CNTs can be characterized using a pair of integers ( $n$  and  $m$ ), which give us the rolling-up direction of the carbon sheet and the nanotube diameter. Thus, depending on the different rolling-up modes, the CNTs can be named as armchair with  $n=m$ , zigzag with  $n=0$  or  $m=0$ , or generally chiral when any other  $n$  and  $m$ . Many of the potential applications of SWNTs and MWNTs are highly dependent on their electronic properties and in this context, their ballistic transport behavior and long electron mean free path have shown their potential as molecular wires. [60]

On the other hand, CNTs exhibit excellent structural flexibility and fluidity and can be bent, collapsed, or deformed into various shapes such as buckles, rings, or fullerene onions, providing a variety of shape-controlled physical properties of the nanostructures. Also by varying the geometric structure of the CNTs one can control electronic properties such as electrical conductivity or electron emission properties, thus providing modified electronic characteristics of the functional devices based on the CNTs.

Organic compounds have been used as templates for the generation of inorganic, organic or biological structures and materials rendering themselves the object of an increasing interest over the last years. In this way, taking into account that CNTs have been synthesized as an array of unprecedented structural, mechanical, and electronic properties, together with their high aspect ratio and surface area, these features have pointed them out as ideal templates for the deposition of a number of different materials on the search of new composite structures with promising properties and applications, offering the structural support that most of the inorganic, organic or biological materials generally lack. [61,62]

This ability to shape materials on a microscopic level is always desired but usually deficient. The formation of these hybrid structures is challenging due to the great application potential they display in many different fields and also from the scientific viewpoint. The application of these materials in useful processes and devices is ensured as soon as their production will be accomplished in a precise, reproducible manner, and if possible at reasonable costs.

Most of the applications proposed for CNTs have been shown to be strongly dependent on the development of strategies for functionalizing, processing and/or assembly of the CNTs themselves, mainly because their surface is rather inert, rendering very difficult any type of the mentioned mechanisms or techniques.

This is the case of a material deposition process onto CNTs, since becomes very difficult to control the final homogeneity. It is therefore important to explore feasible techniques whereby a surface modification would guarantee this material deposition onto the surface of the CNTs as a prior functionalization. Several approaches for functionalization of CNTs that have been developed can be classified as defect-site chemistry, covalent side-wall functionalization and non-covalent functionalization (figure 2).

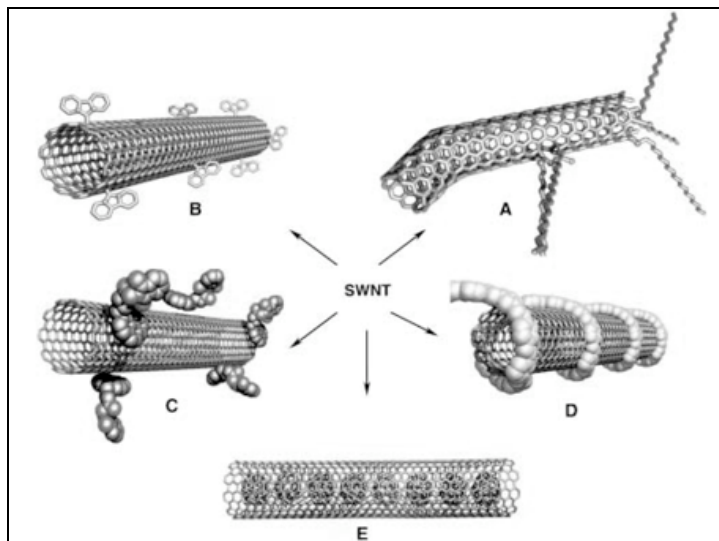


Fig. 2. Different types of SWNTs functionalization: defect-site functionalization (A), covalent sidewall functionalization (B), non-covalent functionalization through, surfactants (C) or wrapping with polymers (D), and endohedral functionalization (E). Reprinted with permission from reference number 64. Copyright 2002 Wiley-VCH.

**Defect-site chemistry** Defect-site chemistry exploits the intrinsic defect sites both at the end and on the sidewalls of the CNTs as a result of the synthetic process. Additionally, the purification process of the CNTs involves the use of strong acids to remove the catalytic particles necessary for the synthesis, due to their oxidative action. This process ends up in holes with oxygenated functional groups like carboxylic acids or alcohol groups among others, which are promising starting points for the attachment of particles, molecular moieties or for further coordination chemistry at these sites.

**Covalent-sidewall functionalization** Covalent-sidewall functionalization is based on the chemical reactivity of the CNTs, related with the pyramidalization of the  $sp^2$ -hybridized carbon atoms and the  $\pi$ -orbital misalignment between adjacent carbon atoms. This pyramidalization and misalignment are scaled inversely with tube diameter, becoming more reactive tubes as decreasing their diameter. This agrees with the fact that fullerenes have a higher reactivity surface (which depends strongly on their curvature) compared to SWNTs which have no strongly curved regions that could serve for direct additions. This statement also explains why side-functionalization of SWNTs by covalent-bond formation needs highly reactive reagent.

**Non-covalent functionalization** Non-covalent functionalization comprises the dispersion of CNTs in aqueous solution, by means of surface active molecules as sodium dodecylsulfate (SDS) or by wrapping them with polymers. While the first one accommodates the CNTs in their hydrophobic interiors (sometimes by strong  $\pi$ - $\pi$  -stacking interactions with the CNT sidewall if the hydrophobic part contains an aromatic group), the second one implies an association of the polymers with the sides of the CNTs based on the hydrophobic thermodynamic preference of CNT-polymer interactions compared to CNT-water interactions, thereby suppressing the hydrophobic surface of the CNTs.

**Endohedral functionalization** Endohedral functionalization comprises the use of the inner cavity of the CNTs for the storage of molecules or compounds since their interaction takes place with the inner surface of the sidewalls, very convenient for confined reactions inside the CNTs.

In summary, defect-side functionalization preserves the electronic structure of the CNTs, since the nanotubes can tolerate a number of defects before losing their unique electronic and mechanical properties. Covalent-sidewall functionalization generates a high degree of functionalization rendering this method very useful for composites formation. However, the destruction of the  $sp^2$ -hybridized structure may result in a loss of thermal conductivity, reducing the maximum buckling force or changing their electronic properties, displaying a semiconductor instead of a metallic behaviour.[63] Finally, the non-covalent functionalization has the main advantage since preserves intact the electronic properties and structure of the CNTs by maintaining the intrinsic nanotube  $sp^2$ -hybridization. [64]

## 2. Nanowires magnetic properties guided by carbon nanotubes

Several methods have been exploited for the synthesis of magnetic colloids on which the magnetic anisotropy can be tuned; relatively simple variations in surfactant composition used to selectively control the growth rates of different faces (in similar procedures as those concerning semiconductor materials [65,66]), [1] assembling previously synthesized magnetic nanoparticles as chains or necklaces, [2-4] [67-69] exploiting electrostatic interactions between the surface charge of magnetic nanoparticles and previously modified carbon nanotubes (CNTs), [70] or depositing the magnetic material on the surface of CNTs in a step-by-step procedure, giving place to homogeneous outer shells.[71] In order to investigate the possibility of obtaining nanowires with a very narrow size distribution and without chemical bonding at the surface we have chosen the third and fourth options schematically illustrated in figure 3. Thus, we have recently demonstrated that driving iron oxide nanoparticles or the direct reduction of nickel salt onto the surface of CNTs (in the second case in the presence of Pt nanoparticles) leads to very homogeneous magnetic nanowires.

### 2.1 Synthetic strategies

#### a. $Fe_3O_4/\gamma\text{-}Fe_2O_3$ -coated CNTs

For this first strategy designed, an assembly of a compact layer of magnetic nanoparticles onto CNTs was taken under consideration. This option was carried out following a procedure that combines the polymer wrapping and LbL self-assembly techniques allowing the non-covalent attachment of iron oxide nanoparticles onto the CNTs and thus leaving intact their structure and electronic properties (see figure 2, D functionalization of CNTs by the polymer wrapping). [72] Poly (Sodium 4-styrene sulfonate) (PSS) was used as the initial wrapping polymer that permits to provide remarkably stable aqueous dispersions of multi-wall carbon nanotubes (MWNTs). Due to the high density of sulfonate groups on this negatively charged polyelectrolyte, the PSS acts as a primer onto the CNTs surface. So that, the subsequent and homogeneous adsorption through electrostatic interactions of a cationic polyelectrolyte, the poly-(dimethyldiallylammonium chloride) (PDDA) is possible, supplying a homogeneous distribution of positive charges. These positive charges ensure the efficient adsorption (exploiting the same phenomenon, by means again of electrostatic interactions) of negatively charged magnetic nanoparticles onto the surface of CNTs.

Although the adsorption of nanoparticles (diameter  $D = 6\text{--}10\text{ nm}$ ) onto CNTs is often problematic due to the extremely high curvature ( $D_{\text{MWCNT}} = 15\text{--}30\text{ nm}$ ) that hinders the formation of dense coatings, the LbL self-assembly technique overcomes these difficulties, basically because of the electrostatic nature of the responsible interactions. [73, 74]

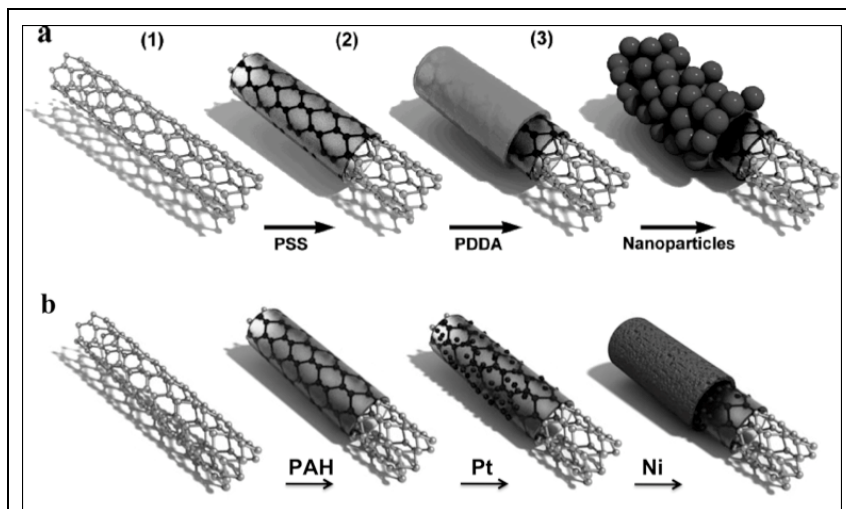


Fig. 3. Schematic illustrations of the synthetic processes used to produce magnetic nanowires using CNTs as guides and supports; a) by driven iron oxide nanoparticles and b) by reducing Ni atoms in a step-by-step process helped by the presence of catalytic Pt sites.

The magnetic nanoparticles prepared in aqueous solution (basic pH) are as mentioned, negatively charged and therefore electrostatically attracted to the positively charged PDDA outer layer adsorbed onto the CNTs. The pH for the most efficient adsorption of the  $\text{Fe}_3\text{O}_4/\gamma\text{-Fe}_2\text{O}_3$  nanoparticles on polyelectrolyte was found to be 11.9–12.0 while at higher pH values no adsorption was observed. A uniform coating of magnetic particles onto the CNTs was achieved, as shown in the TEM images of Figure 4 (a and b) where long ( $> 5\ \mu\text{m}$ ) CNTs appeared completely covered with a dense layer of magnetic nanoparticles. These aqueous dispersions of magnetite/maghemite-coated CNTs were found to be very stable for several days or even weeks in the case of dilute solutions when (after centrifugation/washing) TMAOH (tetramethyl ammonium hydroxide) was added to the solution. Since the early work by Massart, [75] TMAOH has been a popular stabilizer for the preparation of aqueous ferrofluids, mainly comprising iron oxide nanoparticles. The stabilization of these magnetic CNTs in water takes place analogously through the formation of a double layer, with negative hydroxide ions fixed on the surface of the magnetic composites and positive tetramethylammonium as counterions in the basic environment.

Once coated, the magnetic response of these CNTs-based composites was easily and quickly visualized by holding the sample close to a small magnet. Indeed, when a drop of the dispersion was dried on a Si wafer without an external field, the magnetic CNTs were found randomly oriented on the silicon substrate (figure 5a). However, the magnetic CNTs can be oriented in the plane of a silicon wafer by using the mentioned external magnetic field. The magnetite/maghemite-coated CNTs were aligned as long chain structures by means of a

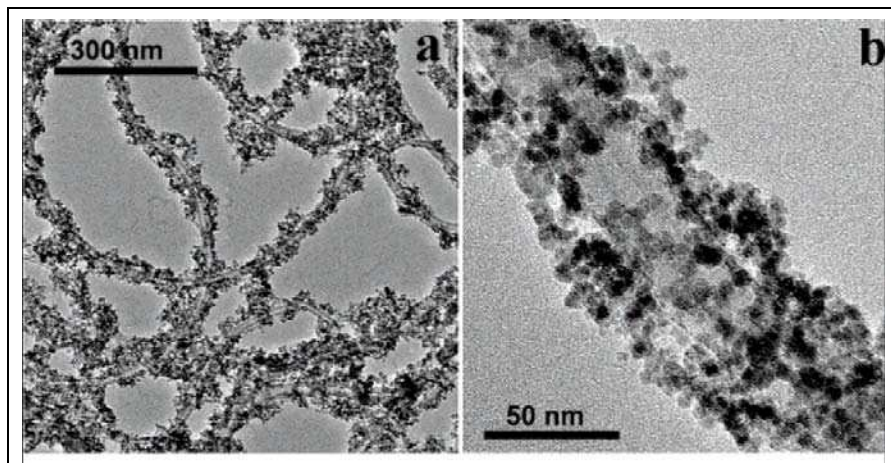


Fig. 4. TEM images at lower (a) and higher (b) magnifications of iron oxide-coated CNTs.

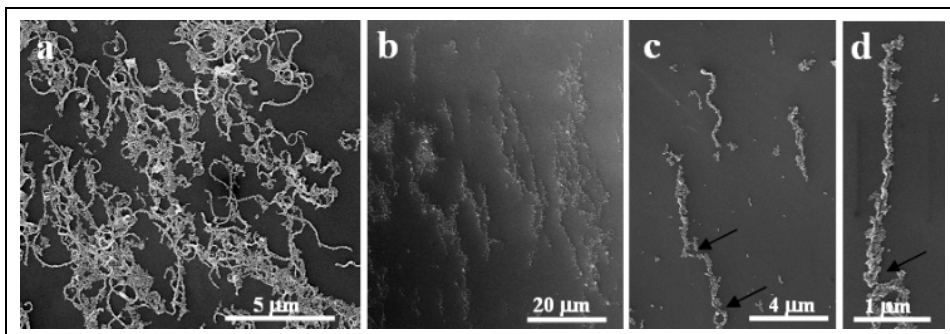


Fig. 5. SEM images of  $\text{Fe}_3\text{O}_4$ -coated CNTs in the absence (a) and in the presence (b,c,d) of an external magnetic field.

magnetophoretic deposition process on the silicon substrate at 300 K, since magnetic CNTs suspended in a liquid align parallel to the direction of the applied magnetic field (in this case under a magnetic field of 0.2T). This fact becomes quite easy to understand as considering that in zero field, the magnetic moments of the iron oxide nanoparticles randomly point in different directions resulting in a vanishing net magnetization (due to the thermal fluctuations able to influence the magnetic moments of the nanoparticle at this temperature). However, if a sufficiently large homogeneous magnetic field is applied, the magnetic moments of the nanoparticles align in parallel and the resulting dipolar interactions are sufficiently large to overcome thermal motion and to reorient the magnetic CNTs favouring the formation of chains of aligned carbon nanotubes. These chain-like structures are formed by connecting the magnetic CNTs in line, touching each other in a head to tail fashion - i.e. north to south pole (at positions indicated by arrows in figure 5c and d).

This behaviour has been reported for different magnetic nanoparticles systems. It takes place due to the anisotropic nature of the dipolar interaction. When comes into play, the north and south poles of the dipolar nanomagnets attract each other while particles coming

close to each other side by side with the magnetization direction parallel will be repelled, thus favoring the formation of nanoparticle chains. [76] Therefore, at first glance one could find astonishing that some magnetic CNTs were found connected in parallel chains (figure 5b). This can be explained by either capillary and van der Waals forces or the fact that long magnetic chains whose end points are not next to each other will also attract each other forming double or triple chains which are parallel and close to each other but are offset to each other along the long axis.

#### b. Ni/NiO-coated CNTs

In the second strategy designed (figure 3b), the synthesis of well-defined, anisotropic magnetic nanotubes, using again the CNTs as templates, was carried out. Again, the  $sp^2$  carbon structure was preserved obtaining in this case a ferromagnetic-like behavior at room temperature. Ni/NiO-coated CNTs/Pt nanocomposites were produced exploiting a stepwise reduction of  $NiCl_2$  using hydrazine, following a procedure that starts with nanocomposites of CNTs previously functionalized with Pt nanoparticles. [77] With this step in mind, a previous CNTs polyelectrolyte functionalization needs to be carried out using another polyelectrolyte, the polyallylamine hydrochloride (PAH). The advantages in this case stem from the fact that ensure the presence of well-dispersed, individual nanotubes and additionally offers a homogeneous distribution of positive charges. This latter distribution of charges drives Pt nanoparticles once present in solution to be deposited onto CNTs.

These Pt nanoparticles were used as catalytic islands so that, the magnetic material can be grown directly on the CNT outer surface in a process that is mediated by this assembled layer of presynthesized, catalytic Pt nanoparticles. This intermediate step yields organic-inorganic hybrid composites that serve as 1D substrates for the preparation of magnetic CNT-supported Ni/NiO nanotubes.

Suspensions of Ni nanowires have also been proposed as magneto-optical switches because of their ability to scatter light that is perpendicularly incident to the wire axis. [78] These nanowires, when ferromagnetic, have large remnant magnetization owing to their large aspect ratios (increased contribution of the shape anisotropy) and hence can be used in low-field environments where superparamagnetic beads do not perform at all. [79] Additionally, since these composite structures involve a Ni/NiO antiferromagnetic/ferromagnetic interface, an exchange bias effect is expected which could find promising applications in magnetoresistive devices. [80]

The deposition of a very uniform and homogenous layer of Ni, without surfactants or other stabilizers in water solution represents a relevant issue since their use would induce a perturbation of the magnetic properties displayed. [42, 81]

Figure 6 shows representative TEM and HRTEM images of the samples produced. These images reflect the homogenous coating of individual CNTs and reveal the multidomain and crystalline nature of the Ni/NiO layers on the final composite. By Fourier transform analysis (of dark field images, not shown), the following intershell and interplanar distances were determined; MWNTs (3.36 Å), Pt (2.19 Å) and Ni (2.03 Å and 1.72 Å), corroborating the envisioned structure of CNTs@Pt/Ni/NiO nanocomposites. The reader has to take into account that CNTs@Pt/Ni nanocomposites were exposed to an oxygen-rich environment during the magnetic material deposition process (aqueous solution) promoting the formation of the chemically stable NiO outer layer around each Ni nanocrystal/nanoshell. [82] This surface passivation process provides the samples with an additional surface stabilization and simultaneously protects the inner metallic Ni from further oxidation. At

this point it can also be underlined the importance of having a continuous shell of a magnetic material onto the CNTs, contrary to the nanocomposites produced on the first strategy, in which the individuality of the iron oxide nanoparticles was kept once deposited onto the CNTs. This has indeed consequences on the magnetic properties displayed, as detailed later on in this chapter.

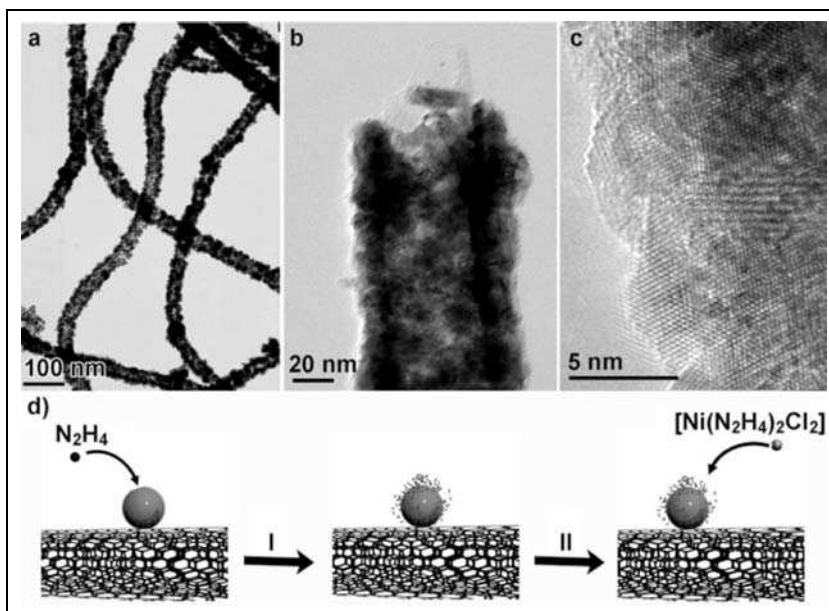


Fig. 6. Representative TEM images of the CNTs@Pt structures coated with a uniform outer layer of Ni/NiO. HRTEM image reflecting the polycrystalline nature of the Ni/NiO layer deposited onto the CNTs@Pt nanocomposites. d) Illustration of Ni reduction on the CNT/Pt side-walls. Step I involves the decomposition of hydrazine on the surface of Pt nanoparticles, which results in a charged surface, and step II the reduction of the hydrazine/Ni complex on the charged Pt surface.

The catalytic behavior of the small Pt nanoparticles play a crucial role in the formation of the metallic Ni on the walls of the CNTs by catalyzing the reduction of the Ni/hydrazine complex formed in aqueous solution, as described below. This reaction allows the CNT/Pt nanocomposites to be coated with a uniform and homogeneous Ni layer (ca. 10 nm thick), with no need for surfactants or other stabilizers in aqueous solution. This feature is relevant since the use of surfactants or other stabilizers usually hinders subsequent manipulation and implementation in different applications. The CNT/Pt@Ni composites are stable in solution (most likely because of the presence of a negatively charged NiO surface layer) and their surface is free of surfactants, thus allowing further functionalization if required. The proposed mechanism for the formation of metallic Ni on the surface of the Pt nanoparticles is depicted schematically in Figure 6d. Complexes between transition-metal ions and hydrazine are easily formed in water. [83] Such complexes can be decomposed in the presence of hydroxy groups, [84] in a process where Ni(II) complexes are reduced to Ni<sup>0</sup>. However, the catalytic decomposition of hydrazine in the presence of Pt nanoparticles can



take place on their surface by an electrophilic addition, that is, by forming electrophilic radicals that can then react with other hydrazine molecules from solution. The presence of metallic platinum nanoparticles therefore implies the reduction of nickel complexes without the need for additional hydroxy groups present in solution. In fact, we observed that reduction of  $\text{Ni}^{2+}$  did not occur in experiments using PAH-functionalized CNTs in the absence of Pt nanoparticles. Thus, the mechanism of Ni nanotube formation can be explained in the following terms: the excess hydrazine that is not complexed with  $\text{Ni}^{2+}$  ions can be catalytically decomposed on the surface of the platinum nanoparticles supported on the CNTs. This step generates a charged metallic surface (step I, Figure 6d) which promotes the reduction of the Ni(II) complex into  $\text{Ni}^0$  (step II, Figure 6d). Subsequent decomposition of hydrazine on the surface of the reduced metal is facilitated, thus favoring further Ni reduction and growth of a homogeneous shell. The process terminates when all the Ni(II) has been reduced. The advantage of this surface-catalyzed reduction of Ni(II) is the formation of a continuous (though polycrystalline) Ni layer rather than an outer shell composed of nanoparticles, with an envisioned improvement of the resulting magnetic properties. Since the CNT/Pt@Ni nanocomposites formed are exposed to an oxygen-containing environment during the deposition of the magnetic material, a stable NiO outer layer is expected to form, passivating the Ni shell and preventing a full oxidation of the magnetic material.<sup>82</sup> However, the presence of nickel oxides on the outer surface of the nickel nanotube could not be confirmed by Fourier transform analysis. To determine whether nickel oxides (and/or hydroxides) were formed on the surface of the CNT/Pt@Ni nanocomposites, the samples were examined by X-ray photoelectron spectroscopy (XPS). Analysis of the Ni 2p peaks revealed a main peak for metallic Ni (852.8 eV) with contributions from different Ni oxidation states, presumably corresponding to the binding energies of NiO and  $\text{Ni}(\text{OH})_2$  (854.4 and 856.5 eV, respectively). These main lines are accompanied by satellite lines with binding energies that are 6 eV higher, which suggests the presence of these Ni oxides at the outer surface of the nickel wires. Apart from passivation, this surface oxidation process leads to ferromagnetic/antiferromagnetic (FM/AFM) interfaces (Ni/NiO), which give rise to an exchange bias effect that increases the potential applications of these nanocomposites, as seen later in the chapter.

## 2.2 Magnetic properties

### a. $\text{Fe}_3\text{O}_4/\gamma\text{-Fe}_2\text{O}_3$ -coated CNTs

In order to check and understand the influence of using CNTs as supports to generate one-dimensional magnetic structures and of the CNTs themselves, the magnetic properties of magnetite/maghemite nanoparticles and the composites were recorded in a Quantum Design Vibrating Sample Magnetometer (VSM). Figure 7 shows hysteresis curves of both structures, collected at 5 K and 300 K, that summarize the typical superparamagnetic behavior. Both iron oxide nanoparticles and magnetic CNTs show the same superparamagnetic behavior, i.e. the same coercive field ( $H_c = 280$  Oe at 5 K) and no remanence or coercivity at room temperature.

At first sight magnetic CNTs seem to have a larger magnetic moment per gram of sample. The saturation magnetization of the original  $\text{Fe}_3\text{O}_4/\gamma\text{-Fe}_2\text{O}_3$  nanoparticles, whose relative concentration cannot be quantified due to the similarity of  $\gamma\text{-Fe}_2\text{O}_3$  and  $\text{Fe}_3\text{O}_4$  XRD spectra present a lower value than the bulk magnetization of  $\gamma\text{-Fe}_2\text{O}_3$  (60-80  $\text{Am}^2/\text{kg}$ ). This was reported to be dependent on the particle size and on the different degree of vacancy

## Thank You for previewing this eBook

You can read the full version of this eBook in different formats:

- HTML (Free /Available to everyone)
- PDF / TXT (Available to V.I.P. members. Free Standard members can access up to 5 PDF/TXT eBooks per month each month)
- Epub & Mobipocket (Exclusive to V.I.P. members)

To download this full book, simply select the format you desire below

